# Soil zymography: Simple and reliable?

## Review of current knowledge and optimization of the method

Bahar S. Razavi[a*], Xuechen Zhang[b,c], Nataliya Bilyera[a,d], Andrey Guber[e], Mohsen Zarebanadkouki[f]

[a] *Department of Soil and Plant microbiome, Institute of Phytopathology, University of Kiel, Kiel, Germany*
[b] *Department of Biogeochemistry of Agroecosystems, University of Göttingen, Göttingen, Germany*
[c] *Department of Agricultural Soil Science, University of Göttingen, Göttingen, Germany*
[d] *Institute of Plant Nutrition and Soil Science, University of Kiel, Kiel, Germany*
[e] *Department of Plant, Soil, and Microbial Sciences, Michigan State University, USA*
[f] *Chair of Soil Physics, University of Bayreuth, Bayreuth, Germany*

*Corresponding author email: brazavi@phytomed.uni-kiel.de

***Abstract***

Within just a few years, soil zymography has become accepted as an attractive and unique approach for 2D mapping of enzyme activities in intact soil samples. With zymography, enzymatic conversion of the substrate into a hydrolysis reaction product can literally be visualized. Soil zymography is, however, fraught with methodical difficulties due to: (i) membrane or gel attachment to the soil surface; (ii) diffusion of substrates through the membrane or gel and of reaction products back to the membrane; (iii) strong effect of imaging (photography) and image analysis on the results. In this review, we describe important procedural details of soil zymography and define the steps necessary to properly visualize enzyme activities in environmental samples. We make the following recommendations to improve zymography results 1) run soil background imaging prior to any soil zymography; 2) confirm that roots are in the soil and not on top of the soil surface; 3) perform soil zymography under the initial environmental conditions of the samples (temperature, water content, light intensity, etc); 4) examine whether membrane/gel attachment during the incubation is appropriate to properly measure enzyme activity; 5) find the right balance between saturating

substrate concentration of soil and selected substrate concentration for zymography; 6) run proper standards to ensure that enzyme activity values can be accurately calculated; 7) fix camera settings and photography conditions; 8) ensure that images are properly analyzed. These steps should help to develop a unified visualization of enzyme activities in soil and ecosystem ecology. Finally, coupling of soil zymography with other imaging techniques and advanced analytical approaches will give insight into the net effect of multiple processes, such as root respiration, rhizodeposition, nutrient and metal(loid) dynamics, plant-mediated oxygen release, microbial respiration and reoxidation of reduced compounds in relation to the activities of enzymes released by plants or microbes.

***Keywords***: *spatial pattern, enzyme distribution, imaging, microbial activity, hotspots*

## 1. Introduction:

### *1.1. Current knowledge and relevance:*

The term 'zymography' denotes the visualization of enzymatic activity by substrate conversion (essentially enzyme photography). The general biochemical reaction can be detected for either the appearance of the reaction product or the disappearance of the substrate (Vandooren et al., 2013; Spohn et al., 2013; Spohn and Kuzyakov 2013). Zymography was first introduced in 1962, for detecting collagen degradation in tadpole tissue and described a matrix metalloproteinase (MMP) (Gross and Lapière 1962; Vandooren et al., 2013). Development of zymography over five decades was mostly focused on the analysis of proteases and their inhibitors in various matrices and media besides soil (Hughes and Herr, 2010; Pan et al., 2011; Choi et al., 2009), for example, to gain insights into tumor formation (Kleiner and Stetlerstevenson, 1994; Nemori and Tachikawa, 1999; Wilkesman and Kurz, 2009).

Kurzbaum et al., (2010), proposed a novel approach to visualize dehydrogenase activity of plant roots by use of tetrazolium violet dye without destructive steps, allowing repeated observations of growing plants and the impact of inhibitors such as sodium azide and cycloheximide.

However, this approach was not tested in soil specimens. Visualization of enzyme activities developed rapidly once fluorescently labeled substrates became widely applied in environmental samples. During the first attempt at visualization of enzyme activity in the soil matrix, the fluorescently labeled substrate was dissolved in agarose solution that was then directly poured onto the sample (Baldrian and Větrovský, 2012). The approach was successful in visualizing the spatial distribution of enzyme activity in soils and in biological specimens such as fungal cell colonies. However, due to the diffusion of the substrate in agar gel, the resolution of this enzyme mapping method was low. The same limitation was visible following the standard zymography assays for the detection of protease and amylase activity in electrophoresis gels (Spohn et al., 2013). The revolutionary optimization of the method started by integrating dissolved fluorescently labeled substrates in membrane filters instead of gels (Spohn and Kuzyakov 2013; Sanaullah et al., 2016; Razavi et al., 2016).

Soil zymography techniques can be utilized for hydrolases or oxidases acting on any biological substrate such as proteins and peptides, oligosaccharides and polysaccharides, lipids and sugars (Kurzbaum et al., 2010; ; Spohn et al., 2013; Voothuluru et al., 2018).

To date soil zymography has been adapted for various applications such as studying the impact of plant species (Razavi et al., 2016), root morphology (Ma et al., 2018), pathogens (Razavi et al., 2017a), abiotic controls like temperature (Ge et al., 2017), drought (Guhr et al., 2015; Ahmadi et al., 2018), nutrient availability (Wei et al., 2018; Giles et al., 2018; Heitkötter and Marschner 2018) and heavy metal pollution (Duan et al., 2018) on the activity of different enzymes in various spheres such as the rhizosphere (Spohn and Kuzyakov 2013; Sanaullah et al., 2016), detritusphere (Spohn and Kuzyakov 2014; Liu et al., 2017; Ma et al. 2017; Wei et al., 2019), and biopores (Hoang et al., 2016; Razavi et al., 2017b), in both lab and field studies (Razavi et al., 2017b). Benefiting from all of these developments, we can now test a larger array of hypotheses related to enzyme-based processes and their roles in biogeochemical cycling. Besides its potential application, the simple sample preparation procedure and relatively worldwide accessibility of all necessary chemicals and equipment have made soil zymography one of the most influential imaging techniques in soil.

Despite the widespread adoption of soil zymography, a comprehensive discussion of the details and pitfalls of the method is not available in the literature. In fact, a major motivation for writing this contribution is that the authors (and our colleagues) receive dozens of inquiries

each year on the execution and interpretation of soil zymography. The prevalent use of high-throughput soil zymography methods has created the need for a comprehensive review of the current state of the art in ecosystem studies. The potential knowledge gap affects the quality and utility of contemporary soil zymography data; distort results or often resulting in relative activity levels that are incomparable among different studies, even though the same enzymes are studied. Methodological optimization will enable the soil and ecological community to perform larger scale meta-analyses, aiming to improve understanding of how plant and microbial enzymes drive ecosystem processes. For specific methodological studies regarding the preparation of calibration lines for soil zymography, and the sensitivity of enzyme activity measurements to exposure time during photography we refer readers to the recent works by Guber et al. (2018a) and Giles et al. (2018).

## 2. Soil zymography and its expected outcomes

Briefly, soil zymography involves visualizing fluorescent compounds produced when a substrate reacts with a substrate-specific enzyme. A membrane filter is soaked in a solution containing a known concentration of fluorescently labeled substrate. The uniformly saturated membrane will be placed in contact with the soil surface either directly (Razavi et al., 2016) or protected by a thin layer of gel (Spohn and Kuzyakov 2013). The membrane will be incubated on the soil surface for a given period of time (see 2.3) and then will be removed and the imprint of the enzyme on the membrane will be imaged under UV light in dark (Fig.1).

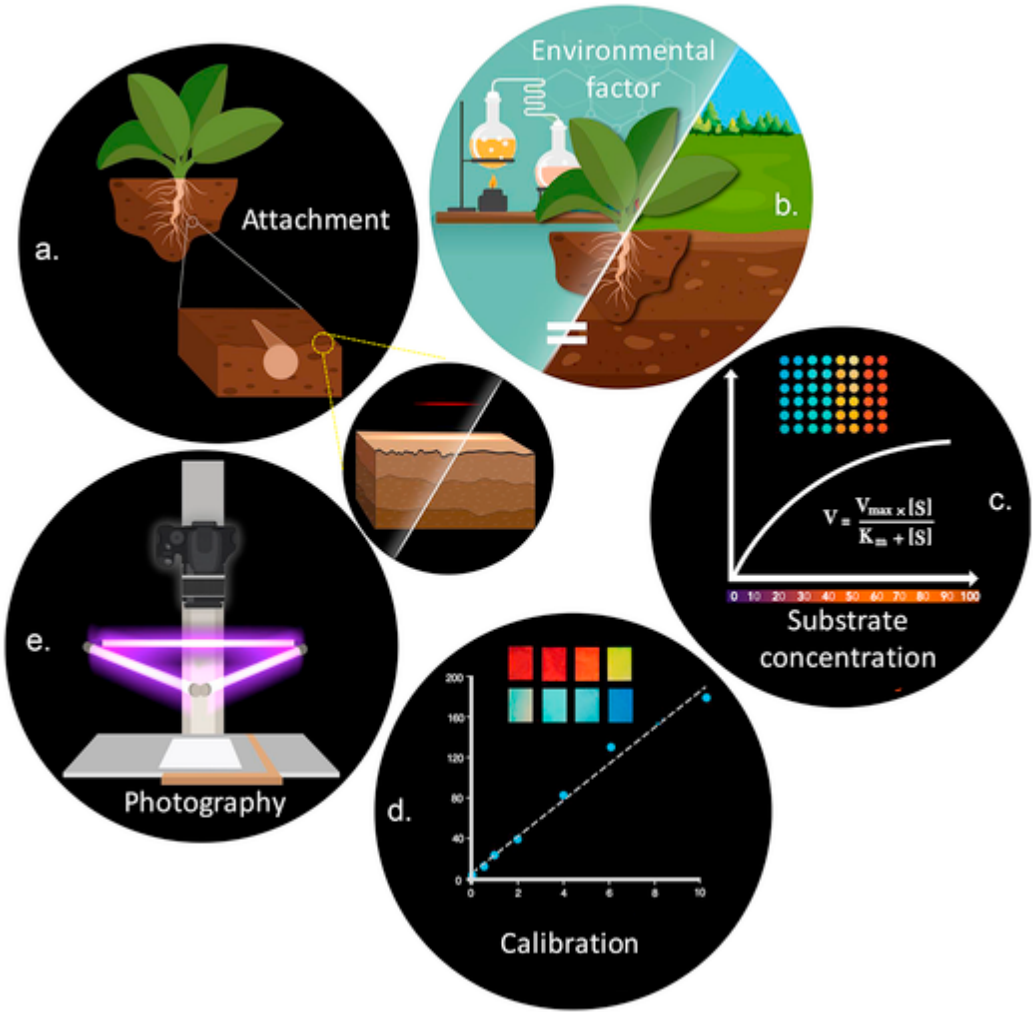


**Fig.1.** Schematic illustration of soil zymography setup and its main steps: a. shows root position and membrane attachment. The inset shows laser scanning for soil surface topography; b. performance of soil zymography under the initial environmental conditions of the samples; c. balance between saturating substrate concentration of soil and selected substrate concentration; d. proper calibration standards; e. fixed camera settings and photography conditions. Art work: Tahoora Emam.

The result of zymography is a 2-D image obtained by a normal camera and is called a zymogram. The captured zymogram can be further quantified and related to the probability that a given enzyme reacts with the substrate and activates its fluorescent agent per unit of area and time. The fluorescent substrate is initially on the membrane and gets activated when it meets a specific enzyme located on the soil surface.

Theoretically, this activation process may occur by two contrasting diffusion-driven processes: i) once a membrane saturated by substrate is placed at the soil surface the substrate may diffuse (by Brownian motion) towards the soil surface. As the substrate meets a specific enzyme at the

soil surface it gets activated. By the nature of diffusion, the now-fluorescent substrate may move back to the membrane, where its imprint will be visualized, ii) another alternative would be that the enzyme at the soil surface diffuses towards the membrane and activates the fluorescent agent of the substrate. Similarly, this process is also Brownian motion driven and may occur in both directions (i.e. the enzyme may return to the soil). After enough time, both processes will reach a steady state and the detected enzyme activity on the membrane will be constant. Although both processes are theoretically possible, the diffusion rates for substrate towards the soil and fluorescent product return is higher. The diffusion rate of a substance is inversely proportional to the square root of its molecular mass. Typically, enzymes have average molecular weights ranging from 10 kD to 2000 kD (Ogston 1962; Wright 1962), while the substrate used in zymography has a molecular weight of 176 D. This simple consideration would suggest that the probability that substrate diffuses towards the soil is surly more than 7.5 times higher than the enzyme towards the membrane ($D \propto \sqrt{1/M}$, where D is the diffusion rate and M is the molecular weight). Thus, in soil zymography, while the membrane is placed on the soil surface it is very probable that the substrate diffuses from the membrane to the soil. This diffusion depends strongly on soil water content at the soil-membrane interface and the contact between soil and the membrane. A partially dried soil surface may adversely affect the results of enzyme activity (consider the case that only the first soil pore at the interface between membrane and soil are dry while the rest of the soil is wetter). In such cases, if the goal is to estimate potential enzyme activity -besides qualitative visualization- soil zymography could be coupled with classical enzyme assays (Hoang et al., 2016; Ma et al., 2017; Zhang et al., 2019).

One of the most important points to consider when performing soil zymography is that it is not a replacement for classical enzyme assays. Classical enzyme assays measure "maximum potential" enzymatic activity (Burns, 1978; Tabatabai and Dick, 2002; Wallenstein and Weintraub, 2008) in soil or litter. By its nature, soil zymography reflects enzyme activity associated with surfaces of a given sample rather than its entire volume (Baldrian and Větrovský 2012). Based on experimental data and simulation it was shown that detected enzyme activity is only a small proportion, around 20-30%, of the actual reactions that take place within the total soil volume (Ma et al., 2017; Guber et al., 2018b).

To ensure that estimations are accurate, several factors must be considered and procedures carried out before starting soil zymography in environmental samples: chemicals and materials,

incubation conditions and duration, imaging conditions, sample preparation and image analysis. We will address each of these in turn with some examples of adaptations for specific conditions; however, for detail methodological descriptions of each hotsphere, in the lab and field, we refer the reader to original experimental studies (Hoang et al., 2016; Razavi et al., 2017b, Liu et al., 2017; Ge et al., 2017).

## 3. Chemicals and materials

### *3.1 Substrate*

Current soil zymography has benefitted greatly from fluorescent dye-conjugated substrates [e.g., 4-methylumbelliferone (MUF), 7-amino-4-methylcoumarin (AMC); Marx et al., 2001; Saiya-Cork et al., 2002] for the detection of many hydrolytic enzymes. These fluorescence agents allow rapid and specific determination of the spatial distribution of enzyme activities involved in C, N, P and S cycling and, thus, provide the opportunity to answer questions related to the enzymatic hotspots on broader scales. Besides MUF- or AMC- conjugated substrates, 1-(3,7-dihydroxyphenoxazin-10-yl) ethanone, (OxiRed) and tetrazolium-dye substrates are also suitable for visualization of enzyme activities. OxiRed ($C_{14}H_{11}NO_4$), is a fluorogenic substrate that can be used to detect peroxidase activity (Table 1). The method is based on determination of a fluorescent signal developed from enzymatic oxidation of the substrate in the presence of peroxidase in the soil. In the presence of horseradish peroxidase (HRP), the OxiRed probe reacts in 1:1 stoichiometry with $H_2O_2$ to produce highly fluorescent resorufin. The substrates can be dissolved in 300µl dimethyl sulfoxide (DMSO) and later diluted with universal buffer to the desired concentration. OxiRed is sensitive to light and oxygen, which makes its application more limited than the other substrates. Tetrazolium violet-based dyes are qualitative redox indicators that enable visualization of dehydrogenase activity (Steponkus and Lanphear 1967; Kurzbaum et al., 2010).

The substrate concentration normally suggested are 10 mM (Spohn et al., 2014) or 10µM (Razavi et al., 2017b). However, these concentrations are not necessarily an optimum concentration for all soil types and, for many soils, concentrations much less than 10 mM or 10µM would be sufficient to reach saturating conditions for each hydrolytic enzyme. The

197 saturated concentration can be inferred from Michaelis-Menten kinetics (Michaelis and Menten,
198 1913).

199 **Table 1.** Enzymes commonly imaged in environmental samples, and their organic matter
200 constituents and substrates

| Enzyme | Synthetic substrate | Organic matter constituent |
|---|---|---|
| β-glucosidase | 4-MUF- β-D-glucopyranoside | Cellulose degradation products |
| β-cellobiosidase | 4-MUF-β-D-cellobioside | Cellulose degradation products |
| α-glucosidase | 4- MUF- β-D-glucopyranoside | Starch degradation products |
| Xylanase | 4-MUF-b-D-xylopyranoside | Hemicellulose degradation products |
| Phosphatase | 4-MUF-Phosphate | Phytate & Phosphodiester bond degrading |
| Leucine-aminopeptidase | L-Leucine-7-amino-4-methylcoumarin | leucine and amino acids |
| Tyrosine-aminopeptidase | L-Tyrosine-7-amido-4methylcoumarin | Tyrosine and amino acids |
| Chitinase | 4-MUF- N-Acetyl-β-D-glucosaminide | Chitin degradation products |
| Chitotriosidase | 4-Nitrophenyl beta-D-N,Nprime, triacetylchitotriose | Chitin degradation products |
| Peroxidase | 1-(3,7-Dihydroxyphenoxazin-10-yl)ethanone | Lignin polymerizing products |

(Modified after German et al., 2011)

201

202 Therefore, pre-testing is necessary to determine the appropriate substrate concentration for the
203 soil prior to zymography. Application of inappropriate concentrations will complicate the
204 interpretation of images, because obtained signals become insensitive to increments of
205 concentration. This results in gray values that are out of the linear part of the calibration curve
206 (over-saturating signals), (Razavi et al., 2016; Guber et al., 2018a), (Fig. 2), (for more detail see
207 section 6.1).

208

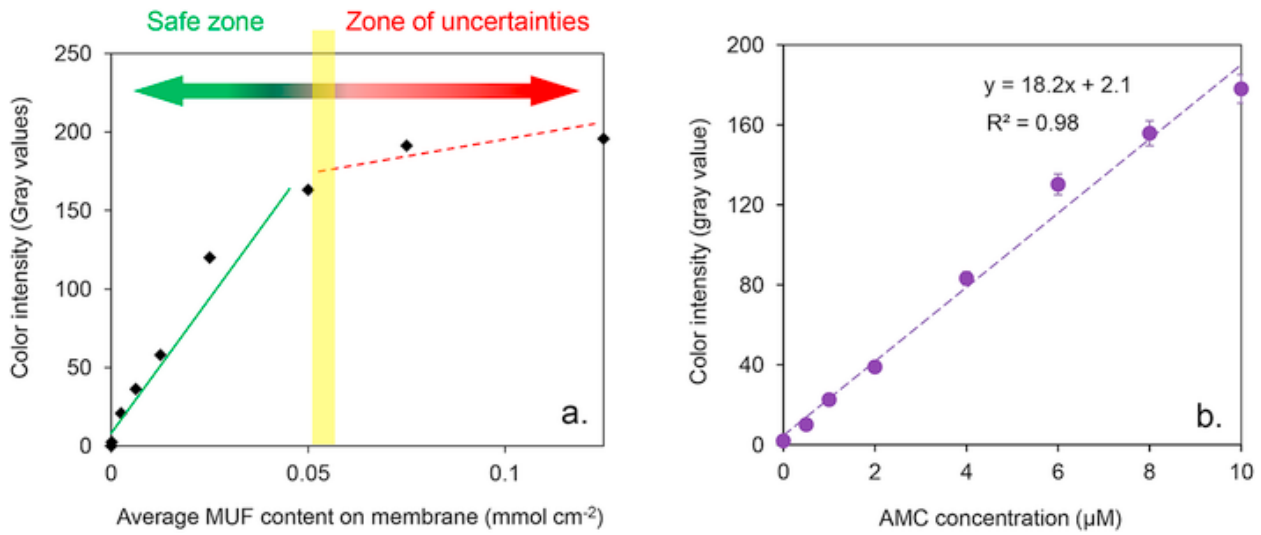


**Fig.2.** Examples of calibration line: a) when the correlation of gray values and concentrations are linear; b) when the correlation is not linear. When the calibration line shows non-linear behavior, the safe zone of the curve according to the concentration and gray values should be identified and only the linear range of the calibration should be used.

*3.2 pH*

Enzymes are sensitive to pH and display specific pH optima (Tabatabai, 1994; Turner, 2010). However, enzymes in soil may not be at their pH optimum (Burns, 1978). Unlike animal digestive tracts, for example, most microbes cannot control the environmental pH for their enzyme activity. Thus, in order to visualize enzyme activities in environmental samples, soil zymography should be run at the same pH as sample. Based on studies of soil enzymology it is known that some of the buffers may interfere with enzyme activity (Burns, 1978; Tabatabai, 1994; German et al., 2011; Sinsabaugh, 2010). For instance, phosphate buffer may interfere with the measurement of phosphatase activities, and is an inhibitor of glucosidase (Dahlqvist, 1968), while citrate can chelate iron (Essington et al., 2005), thereby inhibiting enzymes with iron-heme prosthetic groups (Sinsabaugh, 2010). Besides, MUF- or AMC-conjugated substrates fluoresce best at alkaline pH values (>9; Mead et al., 1955). Since assays are typically conducted at a pH lower than 9, NaOH is often added to raise the pH immediately before reading the samples in a fluorometer (German et al. 2011). Extreme alkalization compromised assay sensitivity because of variation (increase and decrease) in the fluorescence of the product/standard (German et al., 2011). Another issue regarding alkalization is that the

fluorescence of MUF and AMC vary with time following the addition of NaOH (Fig. 3). MUF fluorescence increases until ~20 min after NaOH addition, whereas AMC shows a decrease in fluorescence with time following the alkalization (German et al., 2011). In soil zymography, this would lead to exaggerated/elimination signals, which would be incorrectly, interpreted as high/low enzyme activities on the soil surface or a high/low percentage of hotspots (Fig. 3). It has even been suggested to omit any buffer for enzyme assays (German et al., 2011) or dissolve substrate in sterile water for soil zymography performance (Spohn and Kuzyakov 2014). However, pH fluctuation has been observed in assays performed in the absence of buffer (Fig. 3), (Burns, 1978), while, AMC fluorescence with TRIZMA buffer [$C_4H_{11}NO_3$•HCl, $C_4H_{11}NO_3$ ; pH:7.2] without NaOH addition showed temporal stationary pattern. Therefore, the substrates can be dissolved in any universal buffer that shows a static trend over time and no inhibitory effect on enzymes (Fig. 3).

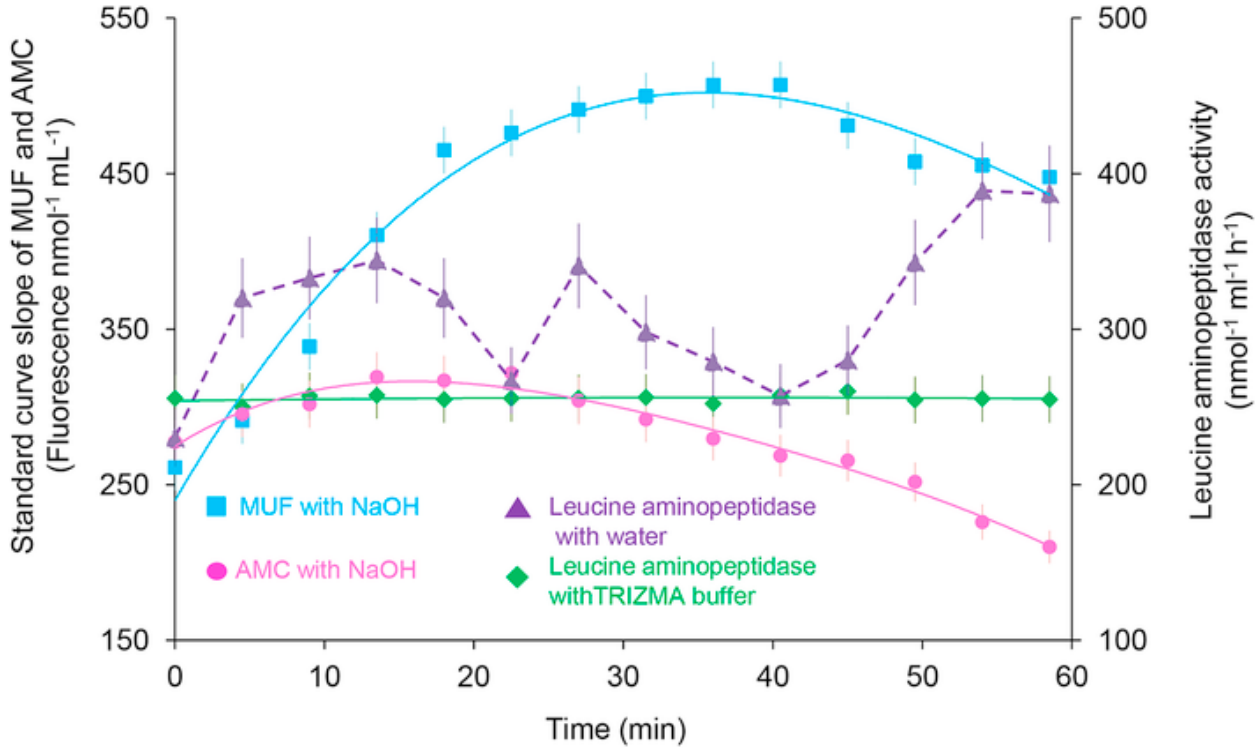


**Fig.3.** Intensity of MUF and AMC standard curves with and without NaOH, as well as trend of leucine aminopeptidase activity with and without buffer.

*3.3 Membranes*

Ideally, the thickness of the membrane filter should be reduced as much as possible to provide uniform vertical distribution of substrate in the membrane. However, thin membranes do not eliminate horizontal diffusion within the membrane, which creates an illusion of a growing area of enzyme activity over time. More specifically, by placing small drops of MUF/AMC with different concentrations in the middle of a membrane saturated with a buffer, followed by monitoring the area of the signal development under UV-light provides sufficient information for estimating the diffusion coefficients. The calculated diffusion coefficient of MUF on a dry membrane filter (Tao Yuan, China) was $5\times10^{-5}$ mm $min^{-1}$. Estimated diffusion coefficients can be used in calculations of expansion of enzyme activity (for example in the rhizosphere).

## 4. Sample preparation

### *4.1. Root position and membrane attachment*

Proper contact between the soil surface and the membrane is crucial for achieving interpretable results. The interpretation of the fluorescent pattern on zymograms is based on the assumption that locations with high fluorescence reflect locations with high enzyme activities on the soil surface, while locations with no fluorescence correspond to locations on the soil surface without activity. However, the contact between the soil surface and membrane depends on the roughness and topology of the soil surface, which varies depending on soil particle size distribution and the positions of roots.

A lack of proper contact between soil surface and membrane may result in the absence of fluorescence signals on the zymograms, and thus, are interpreted as regions with no activity. To reduce the risk of misinterpretation, an initial evaluation of soil heterogeneity by taking and analyzing a photograph of the soil surface and, when possible, performing laser scanning to assess the roughness of the soil surface, is recommended. Laser scanning of the soil surface (e.g. using NextEngine, Inc., Santa Monica, California) prior to zymography could be reasonable for soil surface characterization and micro-topography (e.g. the areas of large and medium-sized soil pores at the surface as well as root distribution), (Guber et al., 2018b). The scanner uses a set of laser beams to hit the soil surface from different angles. Each point from the soil surface is automatically positioned by a laser-light sensor in a 3D coordinate system at a nominal resolution of 1.7 μm (Uteau et al., 2013). While laser scanning provides a detailed soil surface map, it will not yield direct information on which portions of the surface will be in

contact with the membrane after its placement on the surface. The general considerations are that the contact will take place at the areas which have the greatest height (peaks) in comparison with another regions of the soil surface, (Guber et al., 2018b).

The positions of roots on the soil surface is another critical factor that should be considered in performing soil zymography. Generally, there are 4 possible positions for root growth in a rhizobox or in field rhizotrons (root windows) (Fig.4): Roots may be positioned: i) completely on top of the soil surface, ii) partly buried in soil and partly outside of the soil surface, iii) partly buried in soil and positioned at the same level as the soil surface, iv) completely buried in the soil.

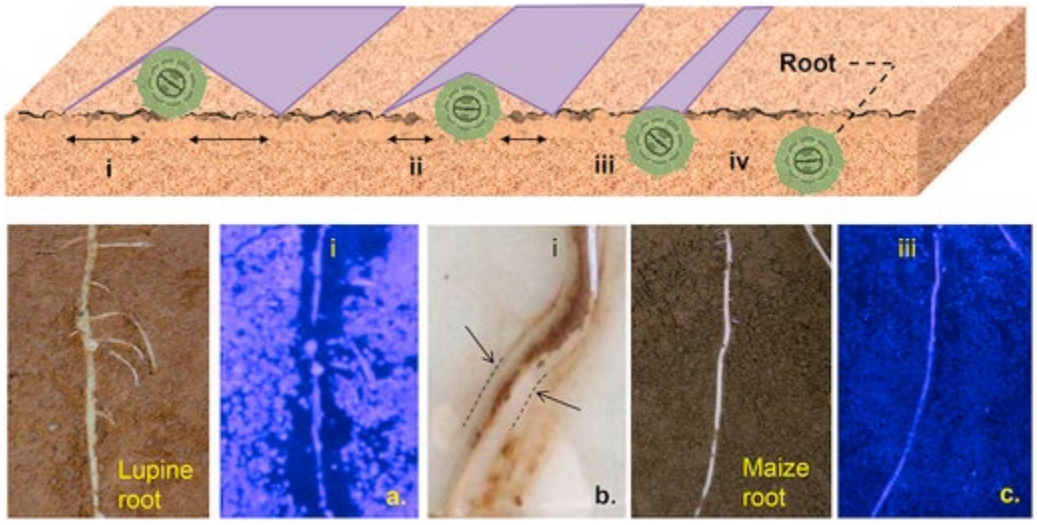


**Fig.4.** Four possible positions of root in soil: i) completely out of the soil surface, ii) partly buried in soil and positioned partly outside of the soil surface, iii) partly buried in soil and positioned at the same level as the soil surface, iv) completely buried in the soil. The eliminated zones around the lupine root (a) corresponding to the similar root position as position (i). (b), shows eliminated zones around the maize root covered by 1 mm gel plate when the root is at a similar position as (i). A clear imprint of enzyme activity on the root and surrounding soil (c) corresponding to the similar root position as (iii). All images are in true color without image processing.

In the case that a root is in position (i), its footprint will be detected on the zymograms, but it should be kept in mind that the contact between the membrane and the surrounding soil will deteriorate depending on the thickness of the root: i.e. a thick root will prevent membrane

contact across a larger region in its surroundings. For the case (ii), the imprint of the root will be detected on the zymograms, but the trail in the surrounding soil will be affected by the thickness of the root standing above the soil surface. Case (iii) is ideal for zymography (Fig.4). The imprint of both roots and the surrounding soil will be detected safely on the zymograms. For the case that the root is in position (iii), its thickness will not have any effect on the contact between membrane and soil surface and its footprint on the zymogram will reflect its enzymatic activity. If roots are completely buried in the soil, (iv), the imprints may not be detected on the zymograms. In this case, the intensity of the detected signal mostly depends on the thickness of the soil layer between the root and membrane (Fig.4). It should be noted that, if the root is located in position (i) or (ii), or the soil surface is not uniform, application of any intervening material e.g. filter paper, gel plate, would not improve the attachment and there will be a "blind spot" around the roots (Fig.4, b). The same is valid for direct application of membrane, as we cannot fold the membrane (Fig.4. a). Thus, confirmation of an appropriate root position is a critical step prior to any soil zymography analysis.

### *4.2. Incubation conditions and duration*

In general, the incubation time depends on the temperature, soil texture, the activity of the tested enzyme in the soil and the soil water content. Soil water content (gravimetric or volumetric water content) and soil texture has a great impact on diffusion of enzyme (Burns et al., 2013). The drier is the soil the longer is the distance that any substrate should diffuse to/from the membrane (the overall chance of enzyme and substrate to diffuse decreases). However, theoretically, diffusion rate will increase at high water content and the probability that substrate would bind to enzyme (form enzyme-substrate complex) will be enhanced (Allison et al., 2011; Manzoni et al., 2012). Hence, the water content of samples should be constant. As the VW refers to the percentage of pores that are filled with water, it would represents the higher portion of enzymes if we assume that enzymes and microorganisms are active in the liquid phase (water-film or biofilms− biosynthesized polymeric substances exude by soil microbiome), (Ekschmitt et al., 2005; Or et al., 2007) or if we assume soil pores serve as conduits for water flow and chemical transport, as well as habitats for microorganisms, and thus play a key role in determining rates and magnitudes of most of soil chemical and biological

processes (Kravchenko et al., 2015). Thus, soil water content has strong effect on results interpretation and accordingly, the incubation time should be long enough for diffusion to take place across the soil surface and the membrane. During this time, it is important to prevent evaporation from the membrane and ensure contact between the membrane and soil surface. To ensure such attachment one may put additional weight onto the membrane. However, different weights will greatly change the obtained signal on the zymograms (Fig. 5). If the load is necessary (for example in case of mapping enzymes around soil columns), then equal weight should be applied to all the samples.

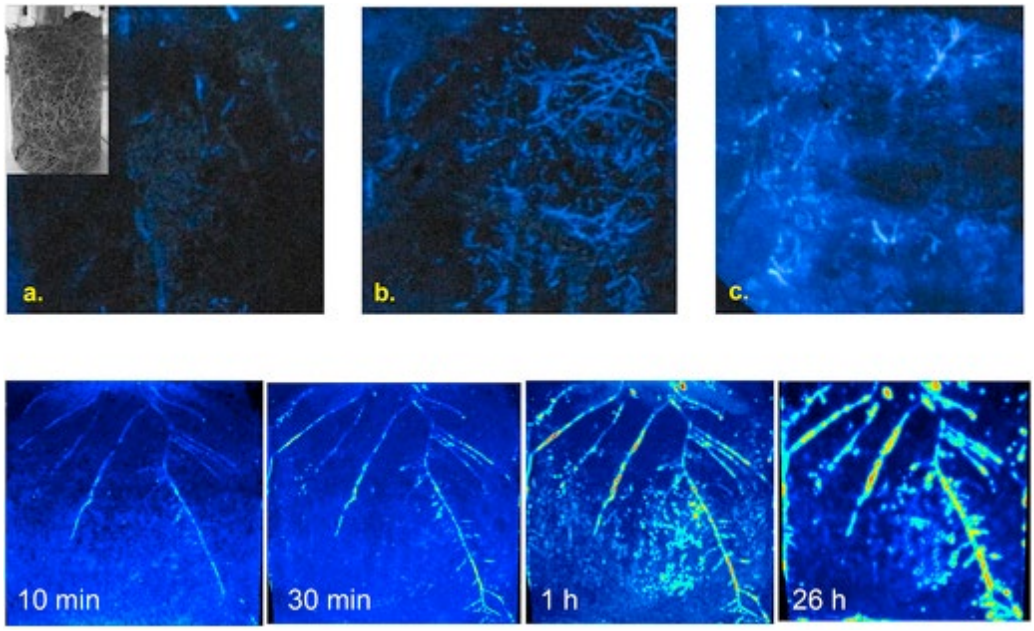


**Fig.5.** Top: a, b and c presenting three different load levels around a soil column. The subfigure of (a) shows real soil column. All images are in true color without image processing. Bottom: four incubation durations. The radial diffusion on the membrane after 26 hours is clearly detectable.

The incubation time should not be too long, as this will cause oversaturation of the membrane. For a coarser soil with lower water content, a longer incubation time would be required than for a wet soil. One hour of incubation is normally selected based on preliminary experiments and previous studies (Dong et al., 2007). The criterion for appropriate incubation time is based on color intensity and diffusion rate: i) reaching the maximum intensity, ii) no detectable horizontal diffusion on the membrane (Fig.5). After incubation, the membranes should be

carefully lifted off the soil surface and any attached soil particles should be gently removed using tweezers. Another option is taking multiple images during the incubation on the soil surface at regular time intervals (2 to 5 minutes) and use the whole image sequence in calculations of enzyme activity.

## 5. Imaging procedure

### *5.1. Camera setting*

The motivation behind this section is to highlight how strongly the imaging step, camera, and the lens models affect the quality of images as well as interpretation of results.

Analyses of over 95 different full-frame models on the Canon EOS 6D – a randomly selected camera – showed the focal length ranged between 12mm to 600mm. These tests revealed that, on average, about 45% of the resolution is lost due to lens defects. The data from DxOMark Image Labs shows that the EOS 6D camera is able to exceed maximum sharpness when paired with the right lens. It should be also taken into account that most digital cameras have internal settings to adjust their capturing properties depending on the intensity of the light received through the lens. In such cases, these settings should be disabled prior to any imaging.

Due to signal variation under different exposure times, the same camera settings should be used for zymograms and calibration standards. For more detailed methodological studies involving the sensitivity of measured enzyme activity to exposure time during photography we refer readers to (Waters, 2009; Guber et al., 2018a; Giles et al., 2018).

### *5.2. Photography*

To obtain reliable results it is very important to perform zymography under the same conditions, such as temperature and selected incubation time. After/during incubation, the membranes will be placed under ultraviolet (UV) illumination with an excitation wavelength of 355 nm and an emission wavelength of 460 nm, in a light-proof room or chamber. The UV light can be a single circular lamp, a rectangle or a square consisting of 3 or 4 similar lamps, with a wattage range of 18 to 22 W. Important is that the sample will receive equal light intensity from all sides (Fig.1).

The distance between the UV light sources, the camera and the samples (zymograms) should be fixed. This includes not only a fixed distance between zymogram, camera and UV light but also camera position, orientation, angle, image capture time and all camera settings. Any light or reflection will have a direct effect on the images and cause overestimation of color intensity. Zymograms should be corrected for the empty membrane ($I_{em}$, zymograms taken without any substrate) and the dark current ($I_{dc}$, the signal recorded by the camera when there is no zymogram) according to (Eq.1):

$$I_{norm} = \frac{I - I_{dc}}{I_{em} - I_{dc}} \quad (1)$$

where $I_{norm}$ is the corrected image and $I$ is the original image. Thus, to correct for variations of the light intensity over the image area, background images from the uncoated membrane as well as background images without any membrane are needed (Eq.1), (Menon et al., 2007). The scaled black flat field (a reference object embedded in all the zymograms) similar in all images should be considered as a reference object during whole image processing (Fig. S1). In addition, we strongly recommend a background test for each individual soil. This includes incubation of a water- or buffer-saturated membrane on the soil and imaging under UV light. This step is indispensable as many soil organic compounds can diffuse into the membrane, as can elements that can be detected as fluorescence under UV light: humic and a reduced quinone-like compounds (quinone compounds can be reduced by cellular reductases), (Watanabe et al., 2004) as well as some heavy metals can produce interfering signals (Fig. 6).

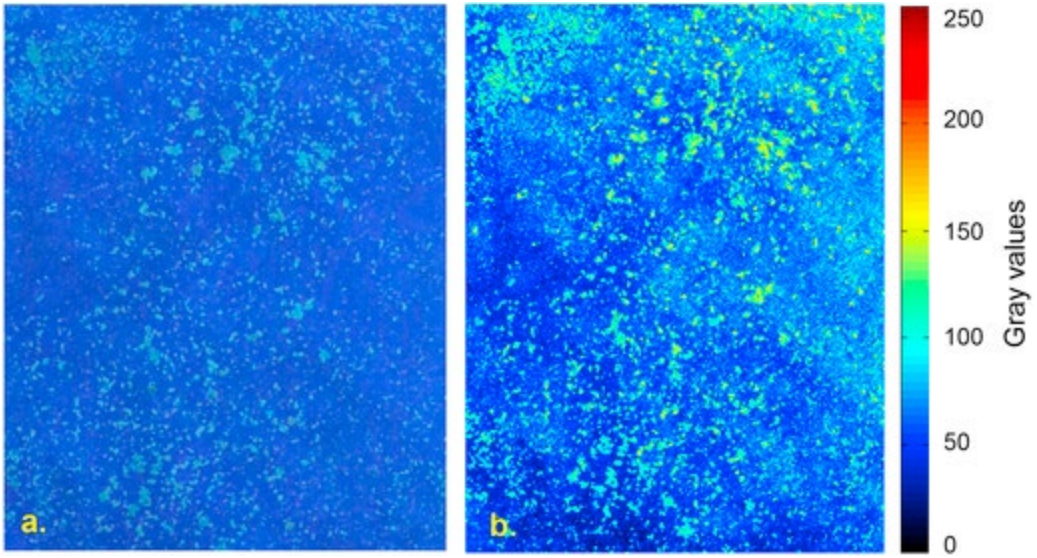


**Fig.6.** Detected false signals on membrane saturated by sterile water under UV light. Not a single pixel refers to spot with enzyme activity. (a) Shows the original zymogram in true color and (b) shows the same zymogram after image processing.

## 6. Image processing, quantification and analysis

### *6.1. Calibration line*

The amount of MUF, AMC or any other fluorogenic conjugate on an area basis can be calculated from the concentration and volume of the solution taken up by the membrane and its size. The membranes used for calibration should be imaged under UV light and analyzed in the same way as the samples (e.g. imaging and light conditions, the same incubation time and same camera settings).

There are two general approaches for calibration of soil zymograms. The simplest consists of saturating the membrane filters with standard MUF/AMC solutions and taking photographs of these filters using the same settings as for the zymography (Spohn and Kuzyakov 2013; 2014). The image obtained with zero concentration of the fluorophore is subtracted from the images with known concentrations (background correction). The concentration of MUF/AMC per unit of area can be calculated for each membrane based on the applied concentration and volume of adsorbed solution. A linear regression with zero intercept is fitted to the obtained values of MUF/AMC (Fig. 2.b). Normally, the correlation of fluorophore concentration and gray values results in an equation as (Eq.2) and is used to calculate enzyme activity per unit of area on zymograms:

$$y=ax+b \quad (2)$$

where y is enzyme activity, x is the grey value of the zymogram, and *a* is the slope of the fitted curve (*For MATLAB script of calibration line please see supplementary materials*). The disadvantage of this approach lies in the deviation of the calibration curves from linearity due to membrane oversaturation at MUF/AMC content of approximately 12mM. Using the calibration beyond this concentration is therefore not reliable (Fig. 2, a).

The second approach applies a known volume of the standard MUF/AMC solution to the membrane surface with continuous imaging. The disadvantage of this approach is the need for many different concentrations and volumes of the standard solutions and a relatively complicated algorithm of pixel-based calibration (Eq.3). The algorithm comprises two sections of linear regression:

$$\begin{cases} \overline{M}_{\mathrm{MUF/AMC}} = b_1 \times \overline{G}; & 0 < \overline{G} < G^* \\ \overline{M}_{\mathrm{MUF/AMC}} = a_2 + b_2 \times \overline{G}; & G^* < \overline{G} \\ b_2 = b_1 - a_2 / G^* \end{cases} \quad (3)$$

where $M_{\mathrm{MUF/AMC}}$ is an average MUF/AMC concentration in the membrane, $a_2$, $b_1$ and $b_2$ are parameters of the linear regression, $G^*$ is the grey value at the breakpoint (Fig. 2. yellow line), and $\overline{G}$ is the grey value averaged across the membrane. The advantage of the second approach is the possibility to extend the calibration curve to larger concentrations of MUF/AMC and overall more accurate calibration due to accounting for non-uniformity in MUF/AMC contents across the membrane (Guber et al., 2018a).

*6.2. Image processing*

Processing zymography images includes 5 steps: 1) transformation of signal (fluorescence) from the images to grayscale values, 2) background correction, 3) root segmentation, 4) root skeletonization, and 5) conversion of grayscale values to enzyme activity.

The intensity of fluorescence is proportional to the activity of the enzyme. To obtain quantitative information, it is possible to process the zymograms using the image processing

toolbox in Matlab (MATLAB, The MathWorks). Zymograms first should be transformed to grayscale images (8, 16 or 32-bit) as matrices and corrected for light variations and camera noise (Eq.1) (Soille 2003; Menon et al., 2007; Zarebanadkouki et al., 2012). Then, the zymograms will be referenced based on the grayscale value received from a reference object embedded in all the zymograms (or scaled black flat field). After referencing the gray values obtained from the zymograms of calibration lines at the concentration of zero can be calculated and then this value will be subtracted from all the zymograms. Note that the same membrane filters should be applied to all of the images, including both zymograms of the samples and the calibration line.

For further analysis, the roots can be easily segmented [cut off from the image by one or more points or lines], due to the strong contrast between the soil and roots. To detect the boundaries of the roots, threshold methods provided by Matlab can be used (Chaudhuri et al., 1989; Hoover et al., 2000). It should be noted that image segmentation is a crucial step in image processing, as it affects all subsequent image analyses (Schlüter et al., 2014). Locally adaptive segmentation methods (e.g. *watershed algorithm*; Beucher and Lantuejoul, 1979) calculate neighborhood statistics for a class assignment in order to smooth object boundaries, avoid noise objects, or compensate for local intensity changes. Due to the added flexibility, local segmentation methods often result in improved segmentation results (Iassonov et al., 2009; Wang et al., 2011). In addition, roots can be segmented and masked by multiplying the zymogram to the mask obtained from root segmentation using the Root-tracker 2D program (Fig. 7, an example Root-tracker image). As the program segments the whole root system, the regions with high enzyme activity can be identified and the noise can be excluded from the analysis (Fig. 7).

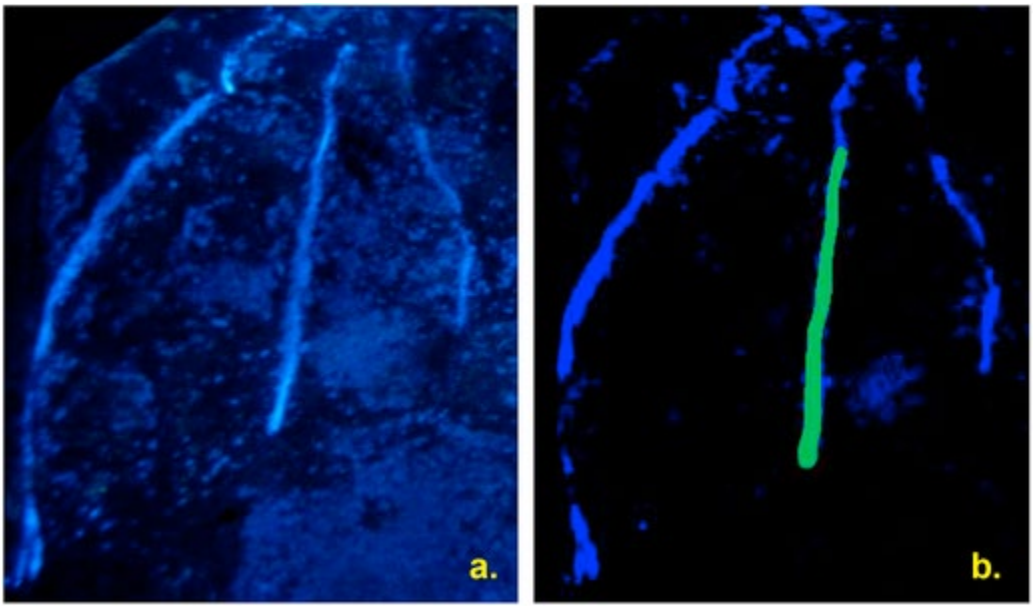


**Fig.7.** (a) Example of zymogram (true color), and (b) shows segmented root in green, while blue is root and noise which should be excluded from the analysis (when the whole root is not visible or the contrast between root and background is not sufficient).

To calculate enzyme activity as a function of distance along the root, the roots that are not overlapping and are entirely visible at the soil surface should be selected (Fig. 7). The images are then skeletonized with a thinning algorithm (Lam et al., 1992). The segmented roots, their lengths, and radii can be calculated using the Euclidean distance map function in Matlab (Menon et al., 2007; Moradi et al., 2011). For the processing of images using ImageJ, we refer readers to (Schlüter et al., 2014).

## 7. Identification, quantification and localization of hotspots

Main relevant biogeochemical processes are take place in the micro-sites, so called hotspots, (Kuzyakov and Blagodatskaya 2015). Hotspots were defined as the small soil volumes with high process rates and very intensive interactions between pools and organisms (Kuzyakov and Blagodatskaya 2015). Hotspots are often defined as a qualitative indicator. Precise definitions vary, with typically the highest 10 to 30% of gray values across the entire image considered as hotspots (Hoang et al., 2016; Liu et al., 2017; Ma et al., 2017; Zhang et al., 2019). Thus, hotspot percentage is an arbitrary value. However, it is valid for the comparison of treatments within

one study, provided that the same threshold is applied to all analyses. In order to unify the calculation of hotspot percentage we recommend the following approach (Kuzyakov and Razavi 2019): First, the mean gray value in the bulk soil and the standard deviation (SD) is calculated. This mean value in the bulk soil is taken as a reference = 1.0 ± SD (Helliwell et al., 2017). Then, moving from the bulk soil to the hotspot, the enzyme activity will increase. The hotspot boundary is accepted as the point at which enzyme activity exceeds + 3 SD. The boundary of + 3 SD is accepted because 99.7% of all bulk soil values are located within ± 3 SD. This approach may provide the most accurate estimation of hotspots according to its original definition (Kuzyakov and Blagodatskaya 2015).

In addition to hotspot identification, it is possible to classify different levels of activity (e.g. very low activity, low activity, moderate activity, and hotspots), (Fig.8). The boundaries of each category can be confirmed by one way analysis of variance (ANOVA). ANOVA can assess the significant differences between independent variables (e.g. mean values of a specific number of adjacent pixels, for example equal to 0.1 mm), (Fig. 8a).

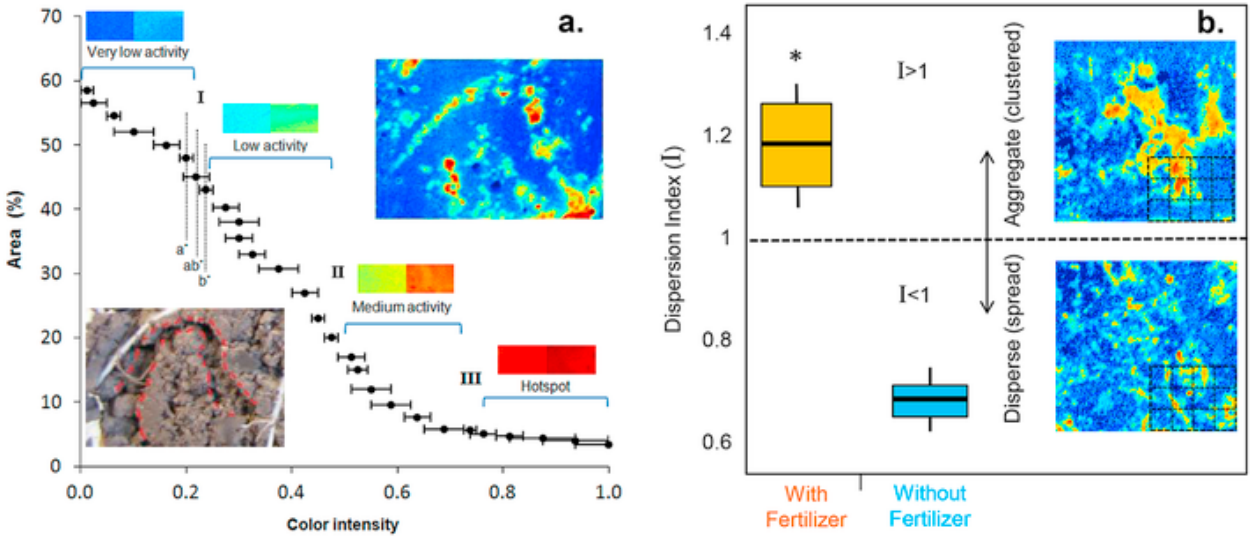


**Fig. 8.** a) Example of detecting the boundaries of different categories of enzyme activities in the specific gradient (biopores). Percentage of the area of MUF/AMC concentration in the total image is considered as a function of color intensity. Asterisks indicate significant differences between the mean values (modified from Hoang et al., 2016). b) Example of spatial distribution of hotspots in soil treated with and without fertilizer. Long-term N fertilization leads to formation of aggregate hotspots while no fertilization caused dispersed distribution of hotspots. The dotted quadrates represent symbolic applied quadrat counts method on images.

Besides, spatial pattern analysis quadrat methods (Diggle, 1983; Arnold et al., 1997) and calculation of dispersion index can illustrate whether the distribution of hotspots in space are aggregated or dispersed (Fig.8b), (Hoang et al., 2016). Spatial point pattern analysis is a statistical method applied to obtain information about the spatial structure of the individual points (hotspots) within a study area (zymogram). There are a number of indices that could be used with the quadrat count method to detect a significant deviation from a Poisson distribution (Fisher et al. 1922). The most common one is dispersion index ($I$) and is defined as:

$$I = \frac{V}{\overline{X}} \quad (4)$$

where V and $\overline{X}$ are the sample variance and the sample mean of the quadrat counts respectively. The method is based on fact that for randomly dispersed points, the variance of the number of points (hotspots) per quadrat is approximately the same as the average number of points per quadrat. Thus, the expected value of the index is $I > 1$ for clustered distribution patterns and $I < 1$ for dispersed spatial distributions (Fig.8b).

Application of spatial point pattern analysis quadrat methods can draw critical conclusions on spatial distribution of hotspots through whole soil profiles with different origins in response to various factors (temperature, time, light intensity, etc.) and promoters (C input, earthworm activities, etc.).

## 8. Coupling zymography with other approaches:

Soil zymography provides information on the spatial distribution of enzyme activities, an important parameter that cannot be obtained with the classical enzyme assay. Soil zymography can be used to answer broader questions by coupling with classical enzyme assays (Hoang et al., 2016; Ma et al., 2017; Zhang et al., 2019) as well as other imaging approaches such as radioisotope imaging (e.g. $^{14}C$, $^{33}P$, $^{35}S$), (Fig. 9), (Spohn and Kuzyakov 2013; Hoang et al., 2017), planar optodes (e.g. $O_2$, $CO_2$, pH), (Fig. 9), FISH (Spohn et al., 2015), neutron radiography, gel-based approaches (e.g. diffusive gradients in thin films (DGT), diffusive equilibration in thin films (DET)), and also with μCT to illuminate spatial distributions of enzyme activities in three dimensions (Kravchenko et al., 2019). The relevance of soil

zymography for soil and ecological sciences is highlighted by the observation that microorganisms use secreted or cell-membrane-bound digestive enzymes to degrade polymeric substances (e.g., cellulose, chitin) and rely on diffusion to access the degradation products (Burns, 1982; Sinsabaugh et al., 1991; Sinsabaugh, 1994). The products of enzymatic degradation (e.g., glucose, amino acids, phosphate) are then used by microorganisms for metabolism and growth. Soil zymography coupled with other imaging techniques as well as molecular approaches (e.g., qPCR) enables *in situ* mapping of all these processes in microsites (hotspots) and hotspheres.

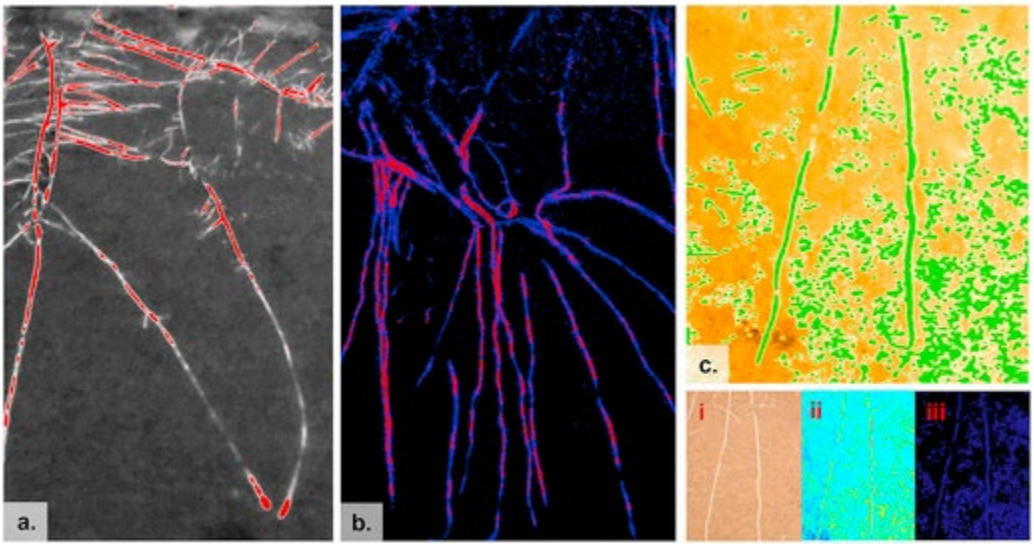


**Fig.9.** a: an example of overlapped $^{14}C$ image and zymography. The red color corresponds to β-glucosidase activity and white represents $^{14}C$ release (root exudate). b: An illustrative example of phosphatase activity (blue) and changes of pH (red) along the maize root. In (a) and (b) background (soil) is converted to black to improve the visibility. c: an example of three overlapped images: real root, zymogram, and $CO_2$ changes. The green color represents the area where leucine-aminopeptidase activity and $CO_2$ release overlapped. Sub-figures shows: i. roots, ii. leucine-aminopeptidase imprint, and iii. $CO_2$ release. There are areas where microbial respiration is visible while imprint of enzyme activity is not detectable (or the activity is low).

## 9. Summary and moving forward:

Clearly, there are many challenges associated with the visualization of enzyme activities in soil and litter. Therefore, we summarized potential abiotic and biotic factors which may distort results (Table 2).

Table 2. Summary of abiotic and biotic factors which may distort results.

| | Factor | Potential effect on result interpretation |
|---|---|---|
| Abiotic | High/Low water content | High/Low enzyme activity |
| | Extra load on membrane | High enzyme activity |
| | Photography exposure time | High/low enzyme activity |
| | Not uniform topography | Disperse hotspot distribution |
| | Root position at soil surface | Localized hotspots around the root |
| | Inappropriate attachment | Aggregate hotspots distribution |
| | Incubation time | Expansion of rhizosphere or hotspots |
| | High/low temperature | High/low overall enzyme activity |
| | High substrate concentration | Outlier enzyme activity |
| | Alkalization | High overall activity for MUF substrates; Low overall activity AMC substrates |
| Biotic | Pathogen infection | Expansion of rhizosphere; High total hotspots% |
| | Fungus contamination | High total hotspots% |
| | Algae contamination | High overall enzyme activity; High total hotspots% |

**Note that the effect of factors is called misinterpretation when they would differ between the initial and incubation conditions or vary between replicates or calibration membranes and zymograms.*

In addition, we would like to conclude with a set of recommendations to improve soil zymography quality and facilitate the sharing of optimization procedures across laboratories: 1) By incubation of water/buffer-saturated membrane on the soil and its photography under UV light (a background test of the soil) prior to any soil zymography, ensure that you are detecting enzyme activity not any other fluorescent compounds.

2) Identify the four possible positions for root growth in the rhizobox or in field rhizotrons and confirm that the roots are in the soil and not on top of the soil, prior to soil zymography.

3) Perform soil zymography under the initial environmental conditions of samples (e.g. keep exactly the same growth temperature, light intensity, water content, etc., while incubating the membrane).

4) Find the balance between saturating substrate concentrations of your soil and substrate concentration for soil zymography.

5) Examine whether attachment during the incubation is appropriate to properly map enzyme activity, and run laser scanning for soil surface topography in advance.

6) Run proper calibration standards to ensure that enzyme activity values are properly calculated.

7) Ensure that camera settings and photography conditions are the same for all samples as well as the measurement of calibration line.

8) Ensure that images are properly analyzed.

If all of these steps are followed, then researchers can be more certain that their images are indeed reflective of the spatial distribution of enzymatic activity in their samples.

Although great efforts have been made toward developing, quantifying and adapting soil zymography, we still have a long way to go. Standardized, user-friendly and correctly interpretable soil zymography tools for non-experts need to be developed and commercialized. The combination of mass spectrometry techniques and soil zymography will ultimately allow the exact trimming pattern of individual substrates by the enzyme (especially proteases) to be determined *in situ* and *in vivo*. Considering how the abiotic environment of the rhizosphere is controlled through a system of feedback loops between roots, microbes, and soil chemistry, in which the dynamics of the microbial community, root exudates, nutrient and elements, enzymes, $O_2$, pH, and $CO_2$ play an essential role, it is clear that coupling soil zymography with other novel approaches will be beneficial. Soil zymography can be used as a mapping tool for localization of microbial hotspots and be coupled further with molecular and microbial analysis to identify the microbial community, or microbial growth and efficiency (Zhang et al., *in preparation*).

Scaling down the soil zymography on a micro-resolution scale or combining soil zymography and other approaches with different scales (for instance nanoSIM) is another untouched side of science that remains as the dark side of the moon to be discovered.

All of these steps will encourage better collaboration among researchers investigating the links between enzyme activities and decomposition. Furthermore, properly estimated enzyme activities may have even more meaning when used in conjunction with functional gene analysis, or emerging proteomic and genomic tools that are expanding our ability to understand microbial decomposers and the significant roles they play in ecosystems (Nannipieri, 2006; Wallenstein and Weintraub, 2008).

## Acknowledgment

BR thanks Prof. Xingliang Xu for the invitation to write this review.

We gratefully acknowledge the German Research Foundation (DFG) for supporting the project: RA3062/3-1 within priority program 2089 and the highlighted importance of imaging approaches to overcome current knowledge gaps between soil, microbiome, and plant scientists. We would like to thank Prof. Yakov Kuzyakov for his valuable comments on the primarily version of the manuscript and Kyle Mason-Jones for the improvement of language and writing style. AG was supported by the National Science Foundation's Long-Term Ecological Research Program (DEB 1027253), by the National Science Foundation's Geobiology and Low-Temperature Geochemistry Program (Award no 1630399), by the Department of Energy Great Lakes Bioenergy Research Center (DOE Office of Science BER DE-FC02-07ER64494).

## References

Ahmadi, K., Razavi, B.S., Maharjan, M., Kuzyakov, Y., Kostka, S.J., Carminati, A., Zarebanadkouki, M., 2018. Effects of rhizosphere wettability on microbial biomass, enzyme activities and localization. Rhizosphere 7, 35–42.

Arnold, S.E., Ruscheinsky, D.D., Han, L.Y., 1997. Further evidence of abnormal cytoarchitecture of the entorhinal cortex in schizophrenia using spatial point pattern analyses. Biological Psychiatry 42, 639–647.

Baldrian, P., Větrovský, T., 2012. Scaling Down the Analysis of Environmental Processes: Monitoring Enzyme Activity in Natural Substrates on a Millimeter Resolution Scale. Applied and Environmental Microbiology. DOI: 10.1128/AEM.07953-11

Beucher, S., Lantuejoul, C., 1979. Use of Watersheds In Contour Detection. International Workshop on Image Processing (Real-time Edge and Motion Detection/Estimation), Rennes, France

Burns, R.G., 1978. Enzyme activity in soil: some theoretical and practical considerations. In: Burns, R.G. (Ed.), Soil Enzymes. Academic Press, London, pp. 295–340.

Burns, R.G., 1982. Enzyme activity in soil: location and a possible role in microbial ecology. Soil Biology and Biochemistry 14, 423–427.

Chaudhuri, S., Chatterjee, S., Katz, N., Nelson, N., Goldbaum, M., 1989. Detection of blood vessels in retinal images using twodimensional matched filters. IEEE Transactions on Medical Imaging 8, 263–269.

Choi, N.S., Kim, B.H., Park, C.S., Han, Y.J., Lee, H.W., Choi, J.H., Lee, S.G., Song, J.J., 2009. Multiple-layer substrate zymography for detection of several enzymes in a single sodium dodecyl sulfate gel. Analytical Chemistry 386, 121–122.

Dahlqvist, A., 1968. Assay of intestinal disaccharidases. Analytical Biochemistry 22, 99–107.

Diggle, P.J., 1983. Statistical Analysis of Spatial Point Patterns. Academic Press, London.

Dong, S., Brooks, D., Jones, M.D., Grayston, S.J., 2007. A method for linking in situ activities of hydrolytic enzymes to associated organisms in forest soils. Soil Biology and Biochemistry 39, 2414–2419.

Duan, C., Fang, L., Yang, C., Chen, W., Cui, Y., Li, S., 2018. Reveal the response of enzyme activities to heavy metals through in situ zymography. Ecotoxicology and Environmental Safety 156, 106–115.

Essington, M.E., Nelson, J.B., Holden, W. L., 2005. Gibbsite and goethite solubility: the influence of 2-ketogluconate and citrate. Soil Science Society of America Journal 69, 996–1008.

Fisher, R.A., Thornton, H.G., Mackenzie, W.A., 1922. The accuracy of theplating method of estimating the density of bacterial populations, with particular reference to the use of Thornton's agar medium with soil samples. Annals of Applied Biology 9, 325–359.

Ge, T.D., Wei, X.M., Razavi, B.S., Zhu, Z.K., Hu, Y.J., Kuzyakov, Y., Jones, D.L., Wu, J.S., 2017. Stability and dynamics of enzyme activity patterns in the rice rhizosphere: effects of plant growth and temperature. Soil Biology and Biochemistry 113, 108–115.

German, D.P., Weintraub, M.N., Grandy, A.S., Lauber, C.L., Rinkes, Z.L., Allison, S.D., 2011. Optimization of hydrolytic and oxidative enzyme methods for ecosystem studies. Soil Biology and Biochemistry 43, 1387–1397.

683 Giles, C.D., Dupuy, L., Boitt, G., Brown, L.K., Condron, L.M., Darch, T., Blackwell, M.S.A.,
684 Menezes-Blackburn, D., Shand, C.A., Stutter, M.I., Lumsdon, D.G., Wendler, R., Cooper,
685 P., Wearing, C., Zhang, H., Haygarth, P.M., George, T.S., 2018. Root development impacts
686 on the distribution of phosphatase activity: Improvements in quantification using soil
687 zymography. Soil Biology and Biochemistry 116, 158–166.

688 Gross, J., Lapiere, C.M., 1962. Proceedings of the National Academy of Sciences of the United
689 States of America, 48, 1014.

690 Guhr, A., Borken, W., Spohn, M., Matzner, E., 2015. Redistribution of soil water by a
691 saprotrophic fungus enhances carbon mineralization. Proceedings of the National Academy
692 of Sciences 112, 14647–14651.

693 Guber, A.K., Kravchenko, A.N., Razavi, B.S., Blagodatskaya, E., Kuzyakov, Y., 2018a.
694 Calibration of 2-D soil zymography for correct analysis of enzyme distribution: Calibration
695 of 2-D soil zymography. European Journal of Soil Science. doi:10.1111/ejss.12744

696 Guber, A., Kravchenko, A., Razavi, B.S., Uteau, D., Peth, S., Blagodatskaya, E., Kuzyakov, Y.,
697 2018b. Quantitative soil zymography: Mechanisms, processes of substrate and enzyme
698 diffusion in porous media. Soil Biology and Biochemistry 127, 156–167.

699 Heitkötter, J., Marschner, B., 2018. Soil zymography as a powerful tool for exploring hotspots
700 and substrate limitation in undisturbed subsoil. Soil Biology and Biochemistry 124, 210–
701 217.

702 Helliwell, J.R., Sturrock, C.J., Mairhofer, S, Craigon, J., Ashton, R.W., Miller, A.J., Whalley,
703 W.R., Mooney, S.J., 2017. The emergent rhizosphere: imaging the development of the
704 porous architecture at the root-soil interface. Scientific Reports 7, 14875, 1–10.

705 Hoang, D.T.T., Pausch, J., Razavi, B.S., Kuzyakova, I., Banfield, C.C., Kuzyakov, Y., 2016.
706 Hotspots of microbial activity induced by earthworm burrows, old root channels, and their
707 combination in subsoil. Biology and Fertility of Soils 52, 1105–1119.

708 Hoang, D.T.T., Razavi, B.S, Kuzyakov, Y., 2017. Revealing hidden effect of earthworm on C
709 distribution and enzyme activity. Geophysical Research Abstracts, 19, EGU2017-13182-1.

710 Hoover, A., Kouznetsova, V., Goldbaum, M., 2000. Locating blood vessels in retinal images by
711 piecewise threshold probing of a matched filter response. IEEE Transactions on Medical
712 Imaging 19, 203–210.

713 Hughes, A.J., Herr, A.E., 2010. Quantitative enzyme activity determination with zeptomole
714 sensitivity by microfluidic gradient-gel zymography. Analytical Chemistry 82, 3803–3811.

715 Iassonov, P., Gebrenegus, T., Tuller, M., 2009. Segmentation of X-ray computed tomography
716 images of porous materials: A crucial step for characterization and quantitative analysis of
717 pore structures. Water Resources Research 45. doi:10.1029/2009WR008087

718 Kleiner, D.E., Stetlerstevenson, W.G., 1994. Quantitative Zymography: Detection of Picogram
719 Quantities of Gelatinases. Analytical Biochemistry 218, 325–329.

720 Kurzbaum, E., Kirzhner, F., Armon, R., 2010. A simple method for dehydrogenase activity
721 visualization of intact plant roots grown in soilless culture using tetrazolium violet. Plant
722 Root 4, 12–16.

723 Kuzyakov, Y., Razavi, B.S., 2019. Rhizosphere size and shape: Temporal dynamics and spatial
724 stationarity. Soil Biology and Biochemistry, https://doi.org/10.1016/j.soilbio.2019.05.011.

725 Kuzyakov, Y., Blagodatskaya, E., 2015. Microbial hotspots and hot moments in soil: Concept
726 and review. Soil Biology and Biochemistry 83, 184–199.

727 Lam, L., Lee, S-W., Suen, C.Y., 1992. Thinning Methodologies-A Comprehensive Survey.
728 IEEE Transactions on Pattern Analysis and Machine Intelligence 14, 869–855.

729 Liu, S., Razavi, B.S., Su, X., Maharjan, M., Zarebanadkouki, M., Blagodatskaya, E., Kuzyakov,
730 Y., 2017. Spatio-temporal patterns of enzyme activities after manure application reflect
731 mechanisms of niche differentiation between plants and microorganisms. Soil Biology and
732 Biochemistry 112, 100–109.

733 Ma, X., Razavi, B.S., Holz, M., Blagodatskaya, E., Kuzyakov, Y., 2017. Warming increases
734 hotspot areas of enzyme activity and shortens the duration of hot moments in the root-
735 detritusphere. Soil Biology and Biochemistry 107, 226–233.

736 Ma, X., Zarebanadkouki, M., Kuzyakov, Y., Blagodatskaya, E., Pausch, J., Razavi, B.S., 2018.
737 Spatial patterns of enzyme activities in the rhizosphere: Effects of root hairs and root
738 radius. Soil Biology and Biochemistry 118, 69–78.

739 Marx, M.-C., Wood, M., Jarvis, S.C., 2001. A microplate fluorimetric assay for the study of
740 enzyme diversity in soils. Soil Biology and Biochemistry 33, 1633–1640.

741 Mead, J.A.R., Smith, J.N., Williams, R.T., 1955. Studies in detoxification. 67. Biosynthesis of
742 the glucuronides of umbelliferone and 4-methylumbelliferone and their use in fluorimetric
743 determination of b-glucuronidase. Biochemical Journal 61, 569–574.

744 Menon, M., Robinson, B., Oswald, S.E., Kaestner, A., Abbaspour, K.C., Lehmann, E., Schulin,
745 R., 2007. Visualization of root growth in heterogeneously contaminated soil using neutron
746 radiography. European journal of soil science 58, 802–810.

747 Michaelis, L., Menten, M.L., 1913. Biorhem. 2. 49, 333–369.

748 Moradi, A.B., Carminati, A., Vetterlein, D., Vontobel, P., Lehmann, E., Weller, U., Hopmans,
749 J.W., Vogel, H.J., Oswald, S.E., 2011. Three-dimensional visualization and quantification
750 of water content in the rhizosphere. New Phytologist 192, 653–663.

751 Nannipieri, P., 2006. Role of stabilised enzymes in microbial ecology and enzyme extraction
752 from soil with potential applications in soil proteomics. In: Nannipieri, P., Smalla, K.
753 (Eds.), Nucleic Acids and Proteins in Soil. Springer, Berlin, pp. 75–94.

754 Nemori, R., Tachikawa, T.A., 1999. Review of in situ zymography: method for localization of
755 protease activities in a tissue. The Tissue Culture Engineering 25, 29–32.

Ogston, A.G., 1962, Molecular Weights of Enzymes Nature 196, 171–172.

Or, D., Phutane, S., Dechesne, A., Ection, S.P.S., 2007. Extracellular Polymeric Substances Affecting Pore-Scale Hydrologic Conditions for Bacterial. Activity in Unsaturated Soils. Vadose Zone 6.

Pan, D., Hill, A.P., Kashou, A., Wilson, K.A., Tan-Wilson, A., 2011. Electrophoretic transfer protein zymography. Analytical Chemistry 411, 277–283.

Razavi, B.S., Zarebanadkouki, M., Blagodatskaya, E., Kuzyakov, Y., 2016. Rhizosphere shape of lentil and maize: spatial distribution of enzyme activities. Soil Biology and Biochemistry 96, 229–237.

Razavi, B.S., Hoang, D.T.T., Blagodatskaya, E., Kuzyakov, Y., 2017a. Mapping the footprint of nematodes in the rhizosphere: cluster root formation and spatial distribution of enzyme activities. Soil Biology and Biochemistry 115, 213–220.

Razavi, B.S., Hoang, D., Kuzyakov, Y., 2017b. Visualization of enzyme activities in earthworm biopores by in situ soil zymography. In: Zymography Methods and Protocols (eds J. Wilkesman & L. Kurz), pp. 229–238. Humana Press, New York, NY, USA

Saiya-Cork, K.R., Sinsabaugh, R.L., Zak, D.R., 2002. The effects of long term nitrogen deposition on extracellular enzyme activity in an Acer saccharum forest soil. Soil Biology and Biochemistry 34, 1309–1315.

Sanaullah, M., Razavi, B.S., Blagodatskaya, E., Kuzyakov, Y., 2016. Spatial distribution and catalytic mechanisms of b-glucosidase activity at the root-soil interface. Biology and Fertility of Soils 52, 505–514.

Schlüter, S., Sheppard, A., Brown, K., Wildenschild, D., 2014. Image processing of multiphase images obtained via X-ray microtomography: A review. Water Resources Research 50, 3615–3639.

Sinsabaugh, R.L., 1994. Enzymatic analysis of microbial pattern and process. Biology and Fertility of Soils 17, 69–74.

Sinsabaugh, R.L., 2010. Phenol oxidase, peroxidase and organic matter dynamics of soil. Soil Biology and Biochemistry 42, 391–404.

Sinsabaugh, R.L., Antibus, R.K., Linkins, A.E., 1991. An enzymic approach to the analysis of microbial activity during plant litter decomposition. Agriculture, Ecosystems & Environment 34, 43–54.

Soille, P., 2003. Morphological Image Analysis: Principles and Applications, 2nd edition, Springer-Verlag, Berlin, Germany, 391 p.

Spohn, M., Carminati, A., Kuzyakov, Y., 2013. Soil zymography - A novel in situ method for mapping distribution of enzyme activity in soil. Soil Biology and Biochemistry 58, 275–280.

792 Spohn, M., Kuzyakov, Y., 2013. Distribution of microbial-and root-derived phosphatase
793 activities in the rhizosphere depending on P availability and C allocation–Coupling soil
794 zymography with $^{14}C$ imaging. Soil Biology and Biochemistry 67, 106–113.

795 Spohn, M., Kuzyakov, Y., 2014. Spatial and temporal dynamics of hotspots of enzyme activity
796 as affected by living and dead roots – A soil zymography analysis. Plant and Soil 79, 67–
797 77.

798 Spohn, M., Treichel, N.S., Cormann, M., Schloter, M., Fischer, D., 2015. Distribution of
799 phosphatase activity and various bacterial phyla in the rhizosphere of Hordeum vulgare L.
800 depending on P availability. Soil Biology and Biochemistry 89, 44–51.

801 Steponkus, P.L., Lanphear, F.O., 1967. Refinement of the Triphenyl Tetrazolium Chloride
802 Method of Determining Cold Injury. Plant Physiology 42, 1423–1426.

803 Tabatabai, M., 1994. Soil enzymes. In: Weaver, R.W., Angle, S., Bottomley, P. (Eds.), Methods
804 of Soil Analysis Part 2: Microbiological and Biochemical Properties. Soil Science Society
805 of America, Madison, pp. 775–833.

806 Tabatabai, M., Dick, W., 2002. Enzymes in soil: research and developments in measuring
807 activities. In: Burns, R.G., Dick, R.P. (Eds.), Enzymes in the Environment. Activity,
808 Ecology and Applications. Marcel Dekker, NewYork, pp. 567–596.

809 Turner, B.L., 2010. Variation in pH optima of hydrolytic enzyme activities in tropical rain
810 forest soils. Applied and Environmental Microbiology 76, 6485–6493.

811 Uteau, D., Pagenkemper, S. K,. Peth, S., Horn, R., 2013. Aggregate and Soil Clod Volume
812 Measurement: A Method Comparison. Soil Science Society of America Journal 77, 60–63.

813 Vandooren, J., Geurts, N., Martens, E., Van den Steen, P.E., Opdenakker, G., 2013.
814 Zymography methods for visualizing hydrolytic enzymes. Nature Methods 10, 211–220.

815 Wallenstein, M.D., Weintraub, M.N., 2008. Emerging tools for measuring and modeling the in
816 situ activity of soil extracellular enzymes. Soil Biology and Biochemistry 40, 2098–2106.

817 Voothuluru, P., Braun, D.M., Boyer, J.S., 2018. An in Vivo Imaging Assay Detects Spatial
818 Variability in Glucose Release from Plant Roots. Plant Physiology 78, 1002–1010.

819 Waters, J.C. 2009. Accuracy and precision in quantitative fluorescence microscopy. The
820 Journal of Cell Biology 185, 1135–1148.

821 Wang, L., Shi, F., Lin, W., Gilmore, J.H., Shen, D., 2011. Automatic segmentation of neonatal
822 images using convex optimization and coupled level sets. NeuroImage 58, 805–817.

823 Watanabe, N., Dickinson, D.A., Liu, R.M., Forman, H.J., 2004. Quinones and Glutathione
824 Metabolism. Methods in Enzymology 378, 319–340.

825 Wei, X., Ge, T., Zhu, Z., Hu, Y., Liu, S., Li, Y., Wu, J., Razavi, B.S., 2018. Expansion of rice
826 enzymatic rhizosphere: temporal dynamics in response to phosphorus and cellulose
827 application. Plant and Soil. doi:10.1007/s11104-018-03902-0

828 Wei, X, Razavi, B.S., Yajun Hu Y, Shen, J., Wu, J., Ge, T., 2019. C/P stoichiometry of dying
829 rice root defines the spatial distribution and dynamics of enzyme activities in root-
830 detritusphere, Biology and Fertility of Soils 55, 251–263.

831 Wilkesman, J., Kurz, L., 2009. Protease analysis by zymography: a review on techniques and
832 patents. Recent Patents on Biotechnology 2009, 175–184.

833 Wright, S.T.C., 1962. An Observation Suggesting that the Molecular Weights of Enzymes can
834 be Arranged in Three Geometric Series, Nature 193, 334–337.

835 Zarebanadkouki, M., Kim, Y.X., Moradi, A.B., Vogel, H.-J., Kaestner, A., Carminati, A., 2012.
836 Quantification and Modeling of Local Root Water Uptake Using Neutron Radiography and
837 Deuterated Water. Vadose Zone Journal, doi:10.2136/vzj2011.0196

838 Zhang, X., Dippold, M.A., Kuzyakov, Y., Razavi, B.S., 2019. Spatial pattern of enzyme
839 activities depends on root exudate composition. Soil Biology and Biochemistry 133, 83–93.